Specific Histone Lysine 4 Methylation Patterns Define TR-Binding Capacity and Differentiate Direct T_3 Responses

Patrice Bilesimo, Pascale Jolivet, Gladys Alfama, Nicolas Buisine, Sebastien Le Mevel, Emmanuelle Havis, Barbara A. Demeneix, and Laurent M. Sachs

Muséum National d'Histoire Naturelle (P.B., P.J., G.A., N.B., S.L.M., E.H., B.A.D., L.M.S.), Département Régulation Développement et Diversité Moléculaire, Unité Mixte de Recherche 7221 Centre National de la Recherche Scientifique (CNRS), Evolution des régulations endocriniennes, 75231 Paris cedex 05, France; and WatchFrog S.A. (P.B.), 91000 Evry, France

The diversity of thyroid hormone T_3 effects *in vivo* makes their molecular analysis particularly challenging. Indeed, the current model of the action of T_3 and its receptors on transcription does not reflect this diversity. Here, T_3-dependent amphibian metamorphosis was exploited to investigate, in an *in vivo* developmental context, how T_3 directly regulates gene expression. Two, direct positively regulated T_3-response genes encoding transcription factors were analyzed: *thyroid hormone receptor* β (*TR*β) and *TH/bZIP*. Reverse transcription-real-time quantitative PCR analysis on *Xenopus tropicalis* tadpole brain and tail fin showed differences in expression levels in premetamorphic tadpoles (lower for *TH/bZIP* than for *TR*β) and differences in induction after T_3 treatment (lower for *TR*β than for *TH/bZIP*). To dissect the mechanisms underlying these differences, chromatin immunoprecipitation was used. T_3 differentially induced RNA polymerase II and histone tail acetylation as a function of transcriptional level. Gene-specific patterns of TR binding were found on the different T_3 -responsive elements (higher for *TR*β than for *TH/bZIP*), correlated with gene-specific modifications of H3K4 methylation (higher for *TR*β than for *TH/bZIP*). Moreover, tissue-specific modifications of H3K27 were found (lower in brain than in tail fin). This first *in vivo* analysis of the association of histone modifications and TR binding/gene activation during vertebrate development for any nuclear receptor indicate that chromatin context of thyroid-responsive elements loci controls the capacity to bind TR through variations in histone H3K4 methylation, and that the histone code, notably H3, contributes to the fine tuning of gene expression that underlies complex physiological T_3 responses. **(*Molecular Endocrinology* 25: 225–237, 2011)**

NURSA Molecule Pages: Nuclear Receptors: TR-α | TR-β;**Ligands:** Thyroid hormone.

Thyroid hormones (THs) regulate multiple developmental and physiological functions in vertebrates. At the cellular level, T_3, the active form of TH, controls cell metabolism, proliferation, and commitment to differentiation or apoptosis. A large part of these regulations is achieved by T_3 binding to the thyroid hormone receptors (TRs). TRs are transcription factors that belong to the subfamily of nuclear receptors (1). TH is a versatile player, not only up-regulating but also down-regulating gene expression.

Current knowledge suggests that both the positive and negative effects of T_3 on gene transcription implicate TRs. To date, most of the studies on the mechanisms of action of TRs have been carried out on positively regulated T_3-response genes. Such studies have shown that TRs bind to specific sequences, thyroid-responsive elements (T_3REs)

ISSN Print 0888-8809 ISSN Online 1944-9917
Printed in U.S.A.

doi: 10.1210/me.2010-0269 Received July 7, 2010. Accepted November 30, 2010.
First Published Online January 14, 2011

Abbreviations: ChIP, Chromatin immunoprecipitation; CZ, control zone; DIMT1L, dimethyladenosine transferase 1 like; GFP, green fluorescent protein; HDM, histone demethylase; NβT, neurotubulin β; qPCR, quantitative PCR; RNA PolII, RNA polymerase II; RT, reverse transcription; RT-qPCR, reverse transcription-quantitative PCR; TH, thyroid hormone; TR, thyroid hormone receptor; T_3RE, thyroid-responsive element; TSS, transcription start site; TZ, transcribed zone.

present in the promoter regions of their target genes. TR-induced transcriptional regulation requires chromatin modification and/or chromatin remodeling. Chromatin modification corresponds to posttranslational modification of N-terminal tail of histones, including a process not limited to acetylation and methylation (2). Such modifications allow control of transcriptional output. Chromatin remodeling will also affect DNA accessibility by localized alteration of nucleosomic structure.

More than a decade ago, a working model was proposed to explain the mechanism of repression by unliganded TR and activation of transcription by liganded TR on positively regulated genes (3). It is still largely valid today. Succinctly, in the absence of T_3, TRs bind T_3REs and recruit a nuclear receptor corepressor complex with histone deacetylase activity, creating a closed chromatin conformation inaccessible to transcriptional machinery and leading to gene repression. T_3 binding induces a conformational change of TR that relieves its inhibitory effect with first, the release of the corepressor complex and second, the recruitment of the steroid receptor coactivator/p300 coactivator complex that contains histone acetyl transferase activity, the SWItch/Sucrose NonFermentable complex involved in chromatin remodeling and the Mediator complex directly involved in transcription activation (4). The resulting chromatin reorganization leads to chromatin opening and gene activation. However, this model cannot explain the physiological diversity of T_3 effects, the understanding of which requires more detailed study of the molecular mechanisms underlying individual gene regulation *in vivo*.

To better understand transcriptional regulation by T_3 in an integrated physiological system, we use the well-studied *Xenopus* metamorphosis model. Anuran amphibian metamorphosis is one of the most striking developmental processes where tadpole transformation is marked by dramatic T_3-induced changes including *de novo* morphogenesis (limbs), tissue remodeling (nervous system), and organ resorption (tail) (5). These changes involve cascades of gene regulation initiated by T_3 and TRs. The diversity of T_3 effects requires tissue- and time-specific control of gene expression leading to the coordination of different transformations at different developmental stages in various organs. The levels of the TR and the localized activities of deiodinases that activate and inactivate TH and determine endogenous T_3 concentrations play important roles in the heterochronic responses of metamorphosis (6). At the single-cell level, the amplitude of direct T_3 responses and the starting-point level of expression need to be controlled to ensure coherent unfolding of the developmental program. The existence of T_3REs with different affinities, the implication of other transcription factors and their binding sites, and varied chromatin landscapes will all contribute to generating differential gene-specific responses to T_3. However, the fact that gene-specific responses are difficult to assess and analyze means that it is, in turn, difficult to derive generalizations about the contribution of various elements to the expression before induction and magnitude of TH responses.

We exploited *in vivo* chromatin immunoprecipitation (ChIP) to address the question of mechanisms of induction of individual, direct-response genes. Expression profiles, binding of TR, recruitment of RNA polymerase II (RNA PolII), and occupancy and function of several histone modifications were investigated on two direct T_3-target genes in the developing brain and tail fin of *Xenopus tropicalis (X. tropicalis*). The genes chosen were *TRβ*, a T_3/TR autoregulated gene and *TH/bZIP*, another rapid T_3-response transcription factor (7, 8). It has already been reported that, in *Xenopus leavis*, the T_3RE in *TRβ* shows a greater affinity for TR than *TH/bZIP* response elements (9) and that individual T_3-response genes have distinct coregulator requirements, the T_3-dependent corepressor to coactivator switch being gene specific (10). Here, we show that these two direct response genes display more differential features including specific magnitude of T_3 responses, gene-specific degrees of repression in absence of ligand, gene-specific dynamics of TR binding levels, and gene-specific chromatin modifications, notably distinct variations in histone lysine methylation. These findings have major implications for our understanding of the fine-tuning and gene-specific actions of T_3-mediated transcriptional control in a vertebrate developmental context and other nuclear receptor mechanisms of action.

Results

TRβ and *TH/bZIP* regulation by T_3 revisited in *X. tropicalis*

Thyroid hormone receptor β (*TRβ*) and basic leucine-zipper thyroid hormone-response gene *(TH/bZIP*) were selected for study because they are two well-known, T_3 direct-response genes in *X. laevis*, with sequenced and characterized promoters, respectively (11, 12). To identify their cDNA sequences and regulatory regions in *X. tropicalis*, a BLAST search was carried out using *X. laevis* sequences (respectively GenBank accession nos. M35361 and U41859 for cDNA and nos. U04675 and AF192491 for promoter). Homologs were found on the *X. tropicalis* genomic scaffold 26 for *TRβ* and 448 for *TH/bZIP* (http://genome.jgi-psf.org/Xentr4/Xentr4.home.html).

The isolated cDNA sequences were used to design primers (Supplemental Fig. 1 published on The Endocrine Society's

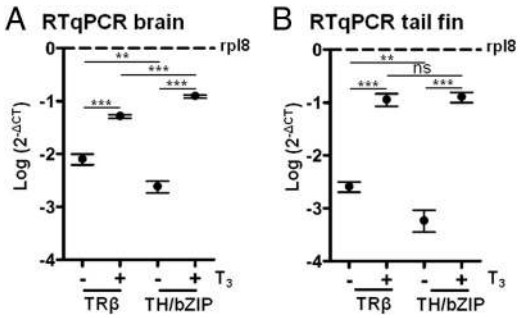

FIG. 1. T_3 induces *TRβ* and *TH/bZIP* transcription. Tadpoles were treated for 48 h with 10 nM T_3. Total RNA was extracted from brain and tail fin and used for RT and real-time qPCR analysis of *TRβ* and *TH/bZIP* (a basic leucine-zipper TH-response gene) expression. Gene expression was normalized against *rpl8* RNA. The data plotted are the log of $2^{-\Delta CT}$ value where ΔCT is the difference between the control gene and the gene of interest. The results represents the mean and SEM of three or six independent experiments. Statistical significance is indicated as not significant (ns); **, $P < 0.01$; or ***, $P < 0.001$.

Journals Online web site at http://mend.endojournals.org) to measure the initial levels of expression and the effects of T_3 treatment on *TRβ* and *TH/bZIP* expression in *X. tropicalis* premetamorphic (stage NF 53) tadpole brain and tail fin by reverse transcription-quantitative PCR (RT-qPCR). *rpl8* was used as a stable internal control gene for normalization, following Normfinder (13) analysis (data not shown). *rpl8* is on scaffold 35 at position 982,964–1,030,015. T_3 treatment significantly increased the mRNA levels of *TRβ* and *TH/bZIP* in brain (Fig. 1A) and tail fin (Fig. 1B), but significant differences between genes were observed. First, and as previously described (12), the initial mRNA levels of *TRβ* were higher than those of *TH/bZIP* in tadpole brain (3.42 ± 0.36-fold; $P < 0.01$) and tail (6.3 ± 2.23-fold; $P < 0.01$) before T_3 treatment. After 48 h of T_3 treatment, mRNA levels of both genes increased significantly ($P < 0.001$; Fig. 1). However, large differences in fold response between the two genes were observed 48 h after T_3 treatment: for *TRβ*, 5.84 ± 0.46-fold in the brain and 43.87 ± 12.95-fold in the tail fin ($P < 0.01$), and for *TH/bZIP* 44.23 ± 2.91-fold in the brain and 144.4 ± 31.35-fold in the tail fin ($P < 0.05$). This result highlights a much stronger effect of T_3 on tail fin than on brain. Finally, at 48 h, the mRNA levels of the two genes differed significantly in the brain (Fig. 1A; higher for *TH/bZIP* than for *TRβ*), but not in tail fin (Fig. 1B). Because *rpl8* expression levels were similar in both tissues in absence and presence of T_3 (data not shown), the expression levels of both genes could be compared between brain and tail fin. The initial mRNA levels of *TRβ* and *TH/bZIP* were higher in tadpole brain than in tail, respectively: 4.26 ± 1.55-fold ($P < 0.01$) and 5.93 ± 2.62-fold ($P < 0.05$), before T_3 treatment.

Next, the T_3REs involved in this regulation were identified using BLAST to compare *X. tropicalis* sequences against *X. laevis TRβ* and *TH/bZIP* regulatory regions, respectively (GenBank accession nos. U04675 and AF192491). In scaffold 26 (*TRβ*), 77 bp with 97% identity were found to contain the T_3RE sequence described in *X. laevis* (Supplemental Fig. 2A). In scaffold 448 (*TH/bZIP*), 190 bp with 95% identity were found to contain the two previously described T_3RE (Supplemental Fig. 2B). One would never be absolutely sure that there are no other bindings sites that may contribute to the regulation. At the level of the T_3REs, which are classical direct repeats with four-nucleotide spacing (DR4), the identity is 100% for both genes (Supplemental Fig. 2, T_3RE highlighted in *bold*). The T_3REs of both genes differ from the consensus DR4 sequence (AGGTCANNNNAGGTCA) by a few nucleotides. TRβ T_3RE has a single nucleotide difference whereas the two *TH/bZIP* T_3REs each have three- and four-nucleotide differences. It seems that, as in *X. laevis*, *TRβ* and *TH/bZIP* are direct T_3-response genes in *X. tropicalis* but both genes behave differently regarding basal levels of expression and mRNA induction after T_3 treatment.

TR recruitment on T_3 response genes

To obtain more direct information on whether these differences in gene expression correlate with TR binding to chromatin, ChIP assays were used. A T_3 treatment period of 48 h was chosen because at this time point both *TRβ* and *TH/bZIP* gene expression is significantly upregulated by T_3 whatever the tissue, presumably with a maximum of cells responding to the stimulus. This is vital when using an *in vivo* model, because maximal homogeneity of the T_3-response in the whole tissue is required. However, the treatments used could be sufficiently long to induce secondary changes that could have indirect and tissue-specific consequences on TR function. Chromatin isolated from control or T_3-treated premetamorphic (stage NF53) *X. tropicalis* tadpole brains and tail fins was immunoprecipitated with an antibody recognizing both TRα and TRβ. The TR-bound DNA fragments were quantified by real-time quantitative PCR (qPCR) (Fig. 2). Two kinds of DNA regions were compared (Fig. 2A for TRβ and Fig. 2B for *TH/bZIP*): the T_3-response promoters containing the transcription start site (TSS) and the TR binding site (T_3RE) and, as a control, a region distant by a few thousand bp from the promoter studied and that was not expected to bind TR [control zone (CZ)]. ChIP without antibody led to the unspecific precipitation of weak amount of DNA in brain (Supplemental Fig. 3A) and in tail fin (Supplemental Fig. 3B). Similar results were obtained when irrelevant antibodies were used (data not shown).

In the absence of T_3, TR was present on the *TRβ*-regulatory region in brain (Fig. 2C) and in tail fin (Fig.

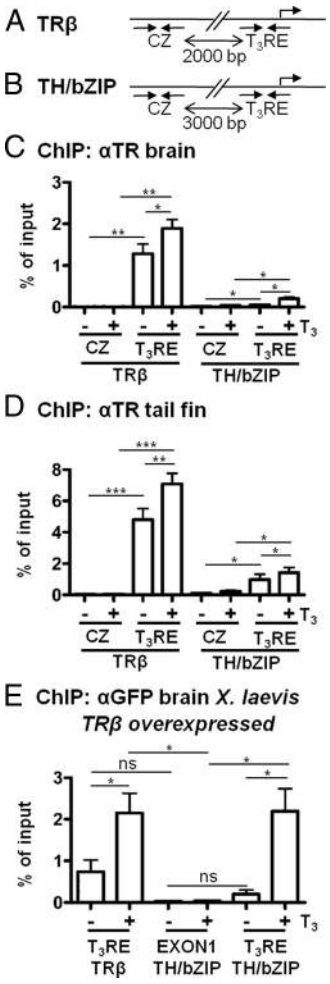

FIG. 2. Effects of T_3 on DNA binding by TR at T_3-response genes. Chromatin isolated from brain or tail fin of T_3-treated *X. tropicalis* tadpoles (10 nM T_3 for 48 h) was immunoprecipitated, and the products were analyzed by qPCR for the presence of T_3RE or an upstream control region (CZ) as schematically represented in panel A for the *TRβ* gene and in panel B for the *TH/bZIP* gene. The distance between the T_3RE area and the CZ area, the position of the primers used for qPCR, and the position of the TSS are also indicated. Sequences are not drawn to scale. C, T_3 increases TR binding to *TRβ* and *TH/bZIP* T_3RE in tadpole brain. Chromatin was immunoprecipitated with antibodies against TR (ChIPαTR). D, T_3 induces TR binding to *TRβ* and *TH/bZIP* T_3RE in tadpole tail fin. Chromatin was immunoprecipitated with antibodies against TR (ChIPαTR). E, TRβ overexpression and TR recruitment on *TRβ* and *TH/bZIP* T_3RE in brain. Chromatin isolated from brain of T_3-treated *X. laevis* transgenic tadpoles overexpressing GFP fused to TRβ in neurons (10 nM T_3 for 48 h) was immunoprecipitated with antibodies against GFP (ChIPαGFP). The product was analyzed by qPCR for the presence of the conserved between *X. tropicalis* and *X. laevis* T_3RE containing region (T_3RE) of *TRβ* and *TH/bZIP* gene. *TH/bZIP* coding locus was used as negative control (Exon1 *TH/bZIP*). The mean values and SEM of four (panels C and D) or three (panel E) independent experiments are expressed as percent of input. Statistical significance as compared with untreated animals is indicated as not significant (ns); *, $P < 0.05$; **, $P < 0.01$; or ***, $P < 0.001$.

2D). As expected, no TR was found on *TRβ* CZ whether from brain (Fig. 2C) or tail fin (Fig. 2D). In the same samples, a weak but significant signal of TR on *TH/bZIP* T_3RE was seen in the brain compared with the CZ (Fig. 2C). In the tail fin, a clear signal of TR on *TH/bZIP* T_3RE was seen (Fig. 2D). After T_3 treatment, TR binding increased significantly on T_3RE region of each gene in both tissues (Fig. 2C for brain and Fig. 2D for tail fin). All these changes observed for TR binding after T_3 treatment were independent of any change in recruitment on CZ for both genes and in both tissues (Fig. 2C for brain and Fig. 2D for tail fin). TR presence was between 8- and 10-fold higher on the *TRβ* T_3RE than on the *TH/bZIP* T_3RE in both tissues analyzed (Fig. 2C for brain, $P < 0.01$; and Fig. 2D for tail fin, $P < 0.001$). Also for each gene, TR presence was also between 3- and 4-fold lower in the brain than in the tail fin [compare Fig. 2, panels C and D: *TRβ* minus T_3 ($P < 0.05$); *TRβ* plus T_3 ($P < 0.01$); *TH/bZIP* minus T_3 ($P < 0.001$); and *TH/bZIP* plus T_3 ($P < 0.01$)].

Our data suggest that in both brain and tail fin only the *TRβ* T_3RE is occupied by the TR expressed during premetamorphosis and that TR recruitment to *TH/bZIP* T_3RE only occurs when either TR expression and or T_3 levels increase during metamorphosis. The premetamorphic level of TR could therefore be a limiting factor for TR binding, implying that T_3-induced TRβ expression is required for the recruitment of TR to certain T_3REs such as *TH/bZIP*. To address this point, TRβ fused to green fluorescent protein (GFP) was overexpressed under the control of the Neuronal tubuline β promoter (NβT) by germinal transgenesis in *X. laevis* tadpole central nervous system. *X. laevis* was used instead of *X. tropicalis* because data regarding TR binding are comparable (our data and Refs. 7 and 9) and transgenesis in *X. laevis* gives higher success rates than in *X. tropicalis*. We used the NβT promoter to drive TRβ-GFP expression because expression from the ubiquitous Cytomegalovirus promoter decreases significantly during metamorphosis (14). Expression of the transgene in the F_1 generation can be controlled by observation of the GFP signal in the central nervous system (15) that allowed establishment of groups with similar levels of transgene expression (16). ChIP assay with antibodies raised against GFP were used to specifically immunoprecipitate exogenous TRβ-bound chromatin from nuclei isolated from control or T_3-treated premetamorphic (stage NF 53) tadpoles brains. The GFP fused TRβ-bound DNA fragments were analyzed by real-time qPCR (Fig. 2E). The presence in the ChIP product of three DNA regions was analyzed: *X. laevis* TRβ and *TH/bZIP* T_3REs and, as a control, a region corresponding to the first exon of *TH/bZIP* (exon1 *TH/bZIP*) distant from the T_3REs studied. As expected, TRβ-GFP was absent from the non-TR-binding zone (exon1 *TH/bZIP*) irrespective of the presence or absence of T_3 (Fig. 2E). In the absence of T_3, TRβ-GFP showed a clear signal on the

TRβ-regulatory region, but only a very low signal on the *TH/bZIP* T_3RE (Fig. 2E) as observed for endogenous TR (Fig. 2C). After T_3 treatment, TR*β*-GFP binding increased significantly on both T_3RE regions (Fig. 2E). Thus, TR*β* overexpression does not result in higher TR binding to the *TH/bZIP* T_3RE region in absence of T_3, but does induce higher liganded TR binding to *TH/bZIP* T_3RE (Fig. 2E).

RNA PolII recruitment and H3K36 methylation differ on individual T_3 response genes

To link TR*β* and *TH/bZIP* mRNA levels with transcriptional status, the presence of RNA PolII on both genes was studied by ChIP. RNA PolII recruitment was analyzed in the genomic regions previously described for *TRβ* (Fig. 3A) and *TH/bZIP* (Fig. 3B), with the T_3REs for both genes being near their TSS (in the middle of the T_3RE for *TRβ* and for *TH/bZIP* the T_3RE is 63 bp upstream the TSS), the CZ not being transcribed and the exons being transcribed [transcribed zone (TZ)]. In tail fin, RNA PolII was significantly recruited in the absence of T_3, on the *TRβ* TSS (Fig. 3C) and on the *TH/bZIP* TSS (Fig. 3D), compared with their respective CZ. After T_3 treatment, RNA PolII recruitment increased on both *TRβ* (Fig. 3C) and *TH/bZIP* T_3REs (Fig. 3D). Similar results were obtained when chromatin was isolated from brain (Supplemental Fig. 4), except that RNA PolII was not significantly recruited on *TH/bZIP* TSS in the absence of T_3 (Supplemental Fig. 4B). Comparing brain and tail fin, the levels and variations of RNA PolII recruitment were correlated with the increase of mRNA levels observed by RT-qPCR. As expected, RNA PolII was absent from the CZ irrespective of the presence of T_3 (for *TRβ* and *TH/bZIP*, Fig. 3, panels C and D, respectively). In the TZ of both genes, the sensitivity of the method did not allow us to detect significant levels of RNA PolII (Fig. 3, C and D).

To analyze further the transcriptional status of *TRβ* and *TH/bZIP* genes, the level of histone H3 trimethylation on lysine 36 (Me3H3K36) was measured. Me3H3K36 generally accumulates on the coding regions of transcribed genes (17). Before T_3 treatment, low levels of Me3H3K36 were seen on the *TRβ* transcribed region, but not on either the CZ or the TSS (Fig. 3E). In the same physiological conditions, Me3H3K36 was not found on any part of the *TH/bZIP* gene (Fig. 3F). After T_3 treatment, Me3H3K36 strongly accumulated, uniquely in the TZ of both genes (for *TRβ* and *TH/bZIP*, Fig. 3, panels E and F, respectively). Thus, there is a strong correlation between RNA PolII recruitment, Me3H3K36 deposition, and transcription levels.

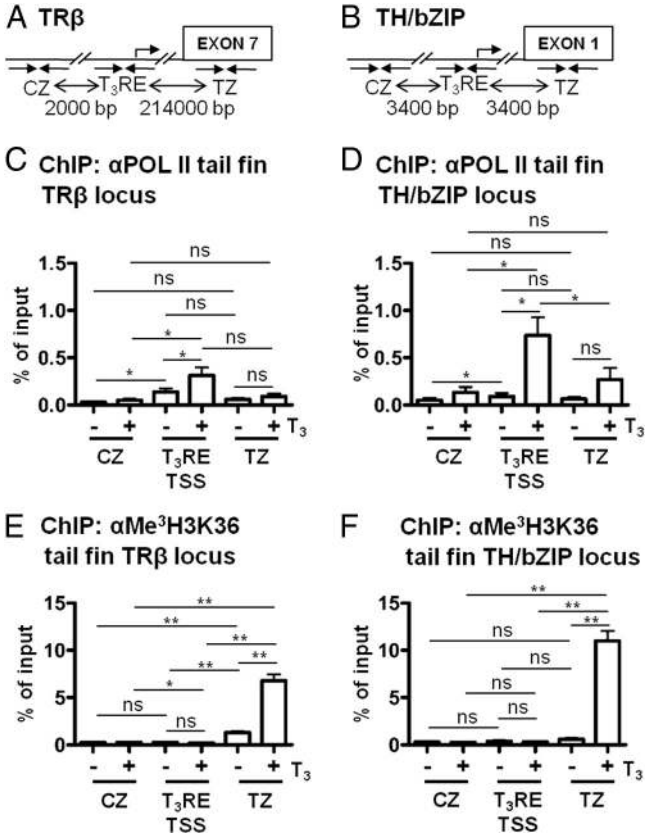

FIG. 3. Effects of T_3 on RNA PolII recruitment and Me3H3K36 occupancy at T_3-response genes. Chromatin isolated from tail fins of T_3-treated *X. tropicalis* tadpoles (10 nM T_3 for 48 h) was immunoprecipitated, and the product was analyzed by qPCR for the presence of the TSS-containing region, which is also the T_3RE-containing region, an upstream control region (CZ), or a coding region (TZ) as schematically represented in panel A for the *TRβ* gene and in panel B for the *TH/bZIP* gene. The distance between each areas and the position of the primers used for qPCR are also indicated. Exonic sequences are *boxed* and intronic or upstream sequences are indicated with *solid line*. Sequences are not drawn to scale. C, T_3 increases RNA PolII recruitment to *TRβ* TSS. Chromatin was immunoprecipitated with antibodies against RNA PolII (ChIPαRNA PolII). D, T_3 induces RNA PolII recruitment to *TH/bZIP* promoter. ChIP was done as described in panel C, but the product was analyzed with primers for *TH/bZIP* genomic regions. E, T_3 increases Me3H3K36 deposition at the *TRβ* transcribed genomic locus. ChIP was done using antibodies against Me3H3K36 (ChIPαMe3H3K36) and primers on *TRβ* genomic locus. F, T_3 induces H3K36 trimethylation at *TH/bZIP*. ChIP was done using antibodies against Me3H3K36 (ChIPαMe3H3K36) and primers for *TH/bZIP* genomic locus. The average values and SEM of four independent experiments are expressed as percent of input. Statistical significance as compared with untreated animals is indicated as not significant (ns); *, $P < 0.05$; or **, $P < 0.01$.

H3 and H4 histone acetylation on T_3-responsive gene promoters

To better understand the molecular mechanisms responsible for the difference in T_3 regulation of direct T_3-response genes, the chromatin states of both the *TRβ* and *TH/bZIP* gene were analyzed. Histone acetylation of the promoters was investigated first, because TR regulation of transcription has been associated with recruitment of

either histone deacetylase activity or histone acetyl transferase activity (10). Using ChIP assay with an antibody specific to pan-acetylated histone H4 (AcH4), ChiP products were analyzed for the presence of the different genomic area already presented in Fig. 2, A and B (for *TRβ* and *TH/bZIP*, respectively). T_3 treatment increased histone H4 acetylation on the *TRβ* and *TH/bZIP* T_3REs in brain (Fig. 4A) and tail fin (Fig. 4B). These increases were specific because they contrast with lack of effect T_3 on AcH4 for dimethyladenosine transferase 1 like (DIMT1L; Supplemental Fig. 5). DIMT1L is a distant housekeeping gene localized on scaffold 87 and is not a T_3-response gene (as revealed with Normfinder analysis; data not shown). For brain and tail fin, AcH4 levels before or after T_3 treatment were similar at TRβ T_3RE. The AcH4 levels were higher at THb/ZIP T_3RE in tail fin compared with brain but the induction rate after T_3 treatment was identical. On the CZ, in both tissues, the level of AcH4 was lower than around the T_3RE for *TRβ* (Fig. 4, A and B) and in the same order of magnitude for *TH/bZIP* (Fig. 4, A and B). Moreover, T_3 treatment increased AcH4 levels on the *TRβ* and *TH/bZIP* CZ in tail fin (Fig. 4B), but not in brain (Fig. 4A).

Histone H3 is another target for NH_2-terminal tail lysine acetylation, and its state reflects gene activation. ChIP with pan-acetylated histone H3 (AcH3) antibodies, revealed high AcH3 occupancy on the *TRβ* T_3RE and *TH/bZIP* T_3RE. T_3 increased AcH3 occupancy significantly for *TRβ* but not for *TH/bZIP* (data not shown). Five H3 lysines can be acetylated, all recognized by the antibody used. Therefore, antibodies recognizing two lysine-specific acetylations were used next: lysines 9 (H3K9) and 18 (H3K18). Looking at the genomic area presented in Fig. 2, A and B, ChIP assays showed no T_3 effect on H3K9 acetylation for either target gene in brain (Fig. 4C). In tail fin, T_3 increased H3K9 acetylation for *TH/bZIP* T_3RE but not for *TRβ* T_3RE (Fig. 4D). T_3 increased H3K18 acetylation on both *TRβ* and *TH/bZIP* T_3REs in brain (Fig. 4E) and tail fin (Fig. 4F). As for AcH3K9, no effects were seen on DIMT1L (Supplemental Fig. 5). Interestingly, AcH3K9 and AcH3K18 occupancies at the *TH/bZIP* CZ in tail fin were also increased by T_3 treatment. Thus, global levels of histone acetylation were positively correlated with levels of gene expression, TR binding, and RNA PolII recruitment.

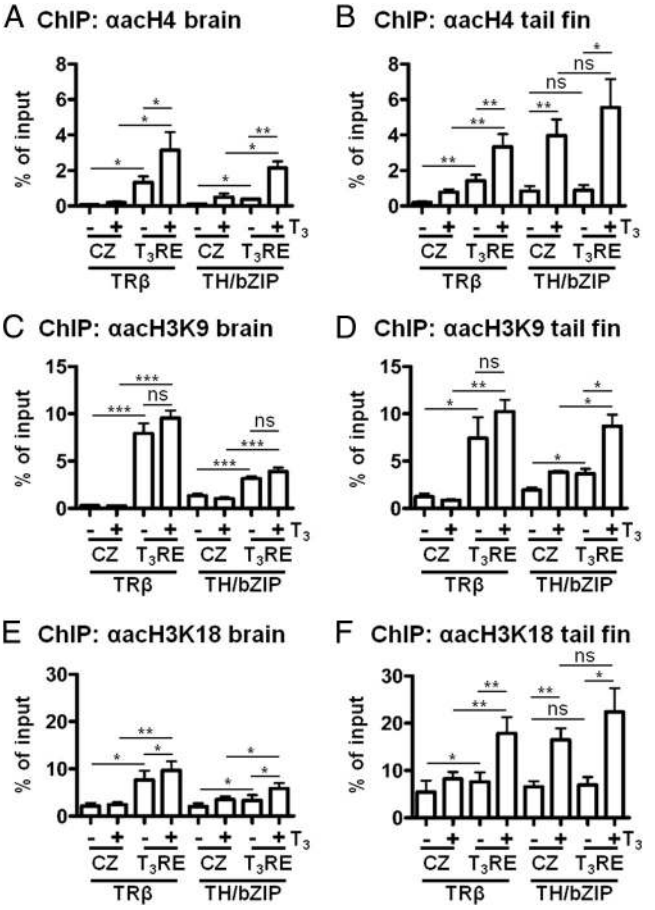

FIG. 4. T_3 treatment effects on histone H3 and H4 acetylation at T_3-response genes. Chromatin isolated from brains or tail fins of T_3-treated tadpoles (10 nM T_3 for 48 h) was immunoprecipitated with antibodies against pan-acetylated histone H4 (AcH4), acetylated histone H3 (AcH3) at lysine 9 (K9) or lysine 18 (K18). ChIP products were analyzed by qPCR for the presence of T_3RE-containing region and CZ region as presented in Fig. 2A for *TRβ* gene and Fig. 2B for *TH/bZIP* gene. A, T_3 increases pan-AcH4 to T_3RE in brain. Chromatin was immunoprecipitated with antibodies against pan-AcH4 (ChIPαAcH4). B, T_3 increases pan-AcH4 to T_3RE in tail fin. ChIP was done with antibodies against pan-AcH4 (ChIPαAcH4). C, T_3 does not affect H3K9 acetylation at T_3RE in brain. ChIP was done using antibodies against AcH3K9 (ChIPαAcH3K9). D, T_3 increases H3K9 acetylation on *TH/bZIP* T_3RE but has no effect on *TRβ* T_3RE in tail fin. Antibodies against AcH3K9 (ChIPαAcH3K9) were used. E, T_3 increases H3K18 acetylation at T_3RE in brain. ChIP was done using antibodies against AcH3K18 (ChIPαAcH3K18). F, T_3 increases T_3RE H3K18 acetylation in tail fin. Chromatin was immunoprecipitated with antibodies against AcH3K18 (ChIPαAcH3K18). The average values and SEM of four independent experiments are expressed as percent of input. Statistical significance as compared with untreated animals is indicated as not significant (ns); *, $P < 0.05$; **, $P < 0.01$; or ***, $P < 0.001$. CZ at least 2000 bp upstream T_3RE area.

Histone methylation status of T_3-response gene promoters

Six major lysine residues (H3K4, H3K9, H3K27, H3K36, H3K79, and H4K20) can be mono-, di-, or trimethylated. Unlike histone lysine acetylation, which is generally coupled to activation, both the position of the lysine residue and the degree of methylation can have different transcriptional consequences (18–20). T_3 effects on the methylation status of lysines 9, 4, and 27 were examined. H3 lysine 9 methylation is associated with closed chromatin and gene repression (18). As shown in Supplemental Fig. 6, trimethylated and dimethylated H3K9 (Me3H3K9 and Me2H3K9, respectively) gave

only weak insignificant signals on *TRβ* and *TH/bZIP* T_3REs and their CZ, independent of T_3 status.

The pattern of H3 methylation at lysine 4 (MeH3K4) is more ambiguous, correlating with either activation or repression (19). ChIP with antibody against mono/di/trimethyl H3K4 on brain, showed T_3 to significantly increase methylation at the *TH/bZIP* T_3RE, but not the *TRβ* T_3RE where the methylation level was already high and T_3 independent (data not shown). To address the specificity of H3K4 methylation, antibodies against dimethyl H3K4 (Me2H3K4) and trimethyl H3K4 (Me3H3K4) were used (Fig. 5, A–D). In both brain and tail fin, T_3 decreased levels of dimethylation on *TRβ* T_3RE (Fig. 5A) and increased it on *TH/bZIP* T_3RE (Fig. 5B). Interestingly, specific differences were seen with Me3H3K4, which was present at high levels on the *TRβ* T_3RE in tail fin (Fig. 5D) and to a lesser extent in brain (Fig. 5C), whereas Me3H3K4 was virtually absent from *TH/bZIP* T_3RE in brain (Fig. 5C) and tail fin (Fig. 5D). T_3 did not modify Me3H3K4 levels. Only the CZ of *TH/bZIP* in tail fin showed any significant levels of H3K4 methylation with no T_3 effects (Fig. 5, A–D).

Finally, the trimethylation of histone H3 at lysine 27 (Me3H3K27), a mark of transcriptional repression (20), was examined. In brain, T_3 treatment decreased slightly the level of Me3H3H27 for *TRβ* whereas it had no effect on *TH/bZIP* T_3RE (Fig. 5E). In tail fin, the levels of Me3H3K27 before T_3 treatment were higher than in the brain for both genes (Fig. 5F). Moreover, T_3 decreased Me3H3K27 occupancy on *TRβ* and *TH/bZIP* T_3REs to reach levels measured in brain (Fig. 5F). Me3H3K27 was observed on DIMTL1 but was not affected by T_3 (Supplemental Fig. 5). At the CZs, the levels of Me3H3K27 without T_3 were in the same order of magnitude as levels at *TRβ* T_3RE and were lower compared with *TH/bZIP* T_3RE (Fig. 5, panel E for brain and panel F for tail fin). Only in tail fin at the *TH/bZIP* CZ, did Me3H3K27 levels decrease significantly after T_3 treatment (Fig. 5F). Thus, as for H3K4 methylation, Me3H3K27 level on *TRβ* and *TH/bZIP* loci showed gene-specific variations and to a lesser extent, tissue specificity.

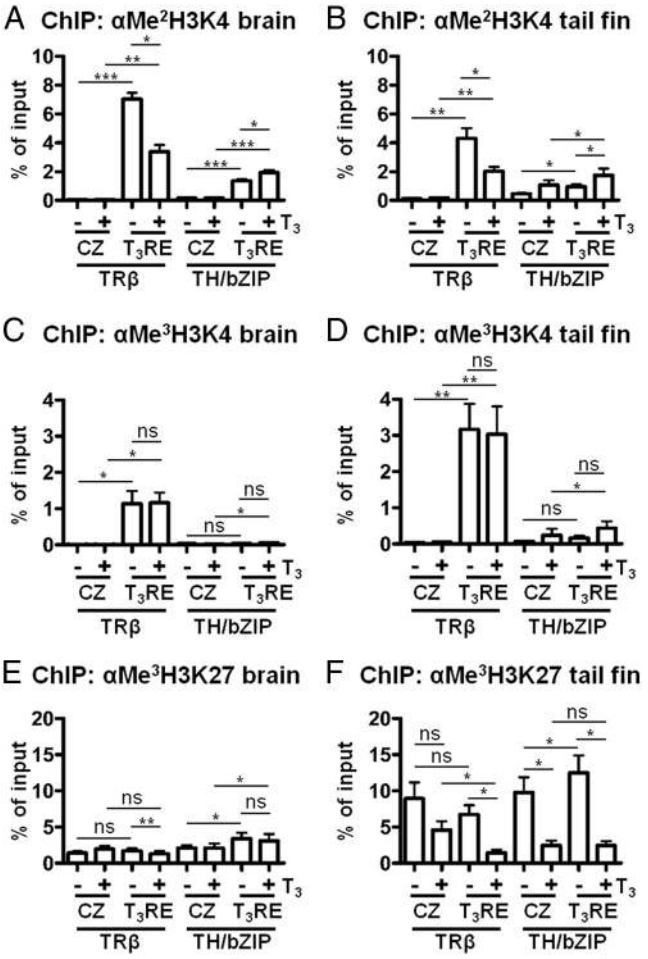

FIG. 5. T_3 treatment effects on histone H3 methylation at T_3-response genes. Chromatin isolated from brains or tail fins of T_3-treated tadpoles (10 nM T_3 for 48 h) was immunoprecipitated with antibodies against dimethyl histone H3 at lysine 4 (Me2H3K4), trimethyl histone H3 at lysine 4 (Me3H3K4), or trimethyl histone H3 at lysine 27 (Me3H3K27). ChIP products were analyzed by qPCR for the presence of T_3RE-containing region and CZ region as presented in Fig. 2A for *TRβ* gene and Fig. 2B for *TH/bZIP* gene. A, In brain, T_3 decreases Me2H3K4 at *TRβ* T_3RE and increases Me2H3K4 at *TH/bZIP* T_3RE. ChIP was done using antibodies against Me2H3K4 (ChIPαMe2H3K4). B, As observed in brain, T_3 decreases Me2H3K4 at *TRβ* T_3RE and increases Me2H3K4 at *TH/bZIP* T_3RE in tail fin. ChIP was done using antibodies against Me2H3K4. C, In brain, Me3H3K4 is present on *TRβ* T_3RE and not on *TH/bZIP* T_3RE with no T_3 effect. ChIP was done using antibodies against Me3H3K4 (ChIPαMe3H3K4). D, In tail fin, Me3H3K4 is present on *TRβ* T_3RE and slightly detected on *TH/bZIP* T_3RE with no T_3 effect. ChIP used antibodies against Me3H3K4. E, In brain, T_3 decreases Me3H3K27 at *TRβ* T_3RE but not on *TH/bZIP* T_3RE. Chromatin was immunoprecipitated with antibodies against Me3H3K27 (ChIPαMe3H3K27). F, T_3 strongly decreases Me3H3K27 occupancy at T_3RE. ChIP was done using antibodies against Me3H3K27. The average values and SEM of four independent experiments are expressed as percent of input. Statistical significance as compared with untreated animals is indicated as not significant (ns); *, $P < 0.05$; or **, $P < 0.01$; or ***, $P < 0.001$. CZ at least 2000 bp upstream from T_3RE area.

T_3-response gene-specific histone demethylase (HDM) and methyltransferase requirements

The differences in H3K4 and H3K27 methylation status for *TRβ* and *TH/bZIP* in response to T_3 suggest a functional interplay between histone methyltransferases and HDMs. Histone methyltransferase and HDM can be targeted to promoters to influence transcriptional status (21). To better understand the requirements of histone lysine modifying enzymes on T_3-response gene regulation, the effect of an HDM inhibitor, pargylin, was investigated. Pargylin is a selective monoamine oxidase inhibitor that also blocks LSD1 (22), the first lysine HDM described (23). However, adding pargylin to aquarium

water led to tadpole death within minutes. Therefore, pargylin was used on cultured tail tips that show similar T_3-induced regression and T_3-target gene responses to those in the whole organism (24).

After 48 h, tail fins were used for RNA extraction and RT-qPCR analysis. *rpl8* was used again as a stable internal control gene for normalization, after Normfinder (13) analysis (data not shown). Its expression was not affected by T_3 and/or pargylin treatment (Supplemental Fig. 7A). As expected, T_3 treatment increased T_3-response gene expression (Fig. 6A). Pargylin treatment alone also increased T_3-response gene expression but to a lesser extent than T_3. To highlight the specific effect of pargylin on T_3-response genes, expression of non T_3-regulated gene was also analyzed. On the four genes used for Normfinder analysis, none of their expressions were affected by the presence of pargylin (Supplemental Fig. 7A). Pargylin+T_3 cotreatment led to increased *TRβ* and *TH/bZIP* mRNA levels. Interestingly, RNA levels after pargylin+T_3 are not different to T_3 alone, suggesting lack of synergy. The results could also indicate that HDM requirement is part of the T_3 regulation processes. ChIP assay on similarly treated tails was used to determine Me2H3K4 and AcH4 levels on *TRβ* and *TH/bZIP* T_3REs. The Me2H3K4 mark was chosen because LSD1 specifically demethylates mono- and dimethylated H3K4 (23). As observed in whole tadpole, in tail culture, T_3 decreased Me2H3K4 on *TRβ* (Fig. 6B), but increased it on *TH/bZIP* (Fig. 6C). Pargylin alone significantly increased Me2H3K4 on *TH/bZIP* (Fig. 6C), but not on *TRβ*, where methylation was unaffected (Fig. 6B). Pargylin and T_3 cotreatment increased Me2H3K4 on *TH/bZIP* (Fig. 6C), but not on *TRβ* (Fig. 6B). Looking at the CZ, pargylin treatment did not change significantly the level of Me2H3K4 marks for either T_3-response gene (Fig. 6, B and C, respectively). No pargylin effects were seen on DIMT1L (Supplemental Fig. 7B).

Pargylin effects on AcH4 were also investigated using ChIP with a pan-AcH4 antibody. In tail fin, T_3, pargylin and T_3+pargylin treatment proportionally increased AcH4 both on the *TRβ* T_3RE (Fig. 6D) and *TH/bZIP* T_3RE (Fig. 6E). These results are in accordance with the increase of *TRβ* and *TH/bZIP* mRNA levels measured in each condition. Moreover, the increase of AcH4 after inhibition of HDM by pargylin, strongly underlines a functional interplay between demethylation and deacetylation.

Finally, as the data showed first, that H3K4 methylation levels correlated with TR binding to T_3RE and second, that pargylin increased H3K4 methylation (at least at *TH/bZIP* T_3RE; Fig. 6C), ChIP assays were used to study the recruitment of TR in tail fin after pargylin treat-

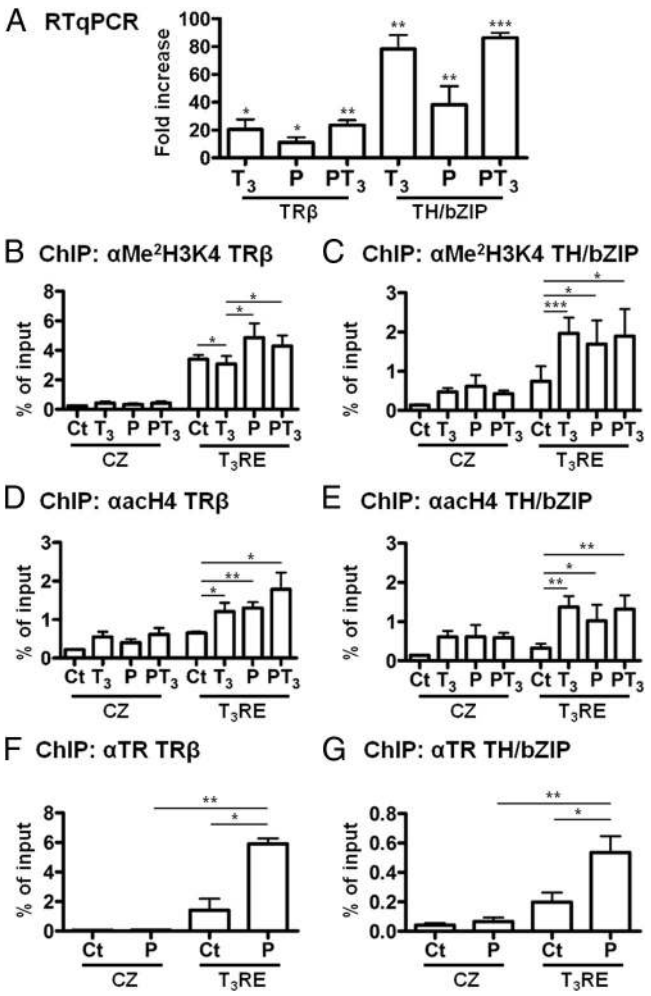

FIG. 6. Pargylin, an inhibitor of HDM, increases T_3-response gene expression and increases TR binding to T_3RE. The tail tips of stage NF 52–53 tadpoles were isolated and placed in cultures dishes. After 48 h with or without 10 nM T_3 and/or 100 nM pargylin (P) for 48 h, tail fins were isolated for RNA extraction or ChIP studies. A, Pargylin treatment increases T_3-response genes expression. The RNA were analyzed by RT-qPCR for the presence of *TRβ* and *TH/bZIP* expression. Gene expressions were normalized against the value for *rpl8* RNA. The average values and SEM of three independent experiments are expressed as multiples of induction, where 1 is equal to expression in the absence of T_3 or pargylin treatment (Ct). B, Effect of T_3 and pargylin treatment on Me2H3K4 occupancy at TR*β* locus. After 2 d of culture, tail fins were isolated from tail explants for chromatin extraction. The presence of Me2H3K4 on T_3RE located near the TSS and 2000 bp upstream the TSS of *TRβ* were analyzed by ChIP (ChIPαMe2H3K4). The average values and SEM of at least four independent experiments are expressed as percent of input. C, T_3 and pargylin effect on *TH/bZIP* T_3RE H3K4 dimethylation. ChIP was done using antibodies against Me2H3K4 and primers around *TH/bZIP* T_3RE and 3000 bp upstream from its TSS. D, T_3 and pargylin increases AcH4 at *TRβ* T_3RE. ChIP was done using antibodies against pan-AcH4 (ChIPαACH4) and primers on *TRβ* T_3RE region and 2000 bp upstream from its TSS. E, T_3 and pargylin effect on AcH4 occupancy at *TH/bZIP* T_3RE. ChIP was done using antibodies against pan-AcH4 and primers around *TH/bZIP* T_3RE and 3000 bp upstream from the TSS. F, Pargylin increases TR recruitment at *TRβ* T_3RE. ChIP was done as using antibodies against TR (ChIPαTR) and primers on *TRβ* T_3RE region. G, Pargylin treatment increases TR binding at *TH/bZIP* T_3RE. ChIP was done using antibodies against TR and primers around *TH/bZIP* T_3RE. Statistical significance as compared with untreated animals is indicated as *, $P < 0.05$; **, $P < 0.01$; or ***, $P < 0.001$. P, Pargylin; Ct, Control tadpoles corresponding to untreated animal.

ment of isolated tail in culture. Pargylin treatment alone significantly increased TR binding on *TRβ* (Fig. 6F) and *TH/bZIP* T_3RE (Fig. 6G). The present data thus show a strong link between H3K4 methylation and TR binding.

Discussion

The current model to explain the mechanism of repression and activation of transcription by TR can be summarized as follows: In the absence of ligand, TR, constitutively present on the T_3RE, can repress gene expression by recruiting a corepressor complex, whereas liganded TR recruits coactivator complexes for gene activation. Corepressor and coactivator complexes induce chromatin remodeling to mediate TR regulation of transcription with special emphasis on histone acetylation. The data reported here allow us to modify this conceptual model. Our results highlight first, that initial premetamorphic expression levels of direct T_3-responses gene are gene specific and dictate the magnitude of regulation by T_3. Second, although both genes have similar TR binding sites, the TR occupancy on T_3RE differs, indicating that TR binding to DNA in the absence of hormone is not a obligatory phenomenon. Third, the variations of AcH4 and AcH3K18 levels are in agreement with the basic model for TR action on positively regulated genes. However, the pattern of AcH3K9 modification is gene and tissue specific with no clear correlation with gene expression. Future studies will be necessary to test the role of this histone mark. Fourth, Me3H3K27 levels negatively correlate with the level of gene expression. Finally, direct T_3-response gene specificity corresponds to a complex pattern of H3K4 methylation strongly linked to TR binding. This methylation mark thus represents a fundamental controller of TR recruitment, permitting fine tuning of transcription. We propose that these diverse molecular codes could be the key to differential modulation of the sensitivity of T_3-response genes in a physiological context. Promoter-specific regulation is particularly interesting in the context of metamorphosis. Potentially, the different gene-regulatory mechanisms could be correlated with the multiple T_3-induced cellular responses underlying tissue remodeling during this complex developmental phenomenon.

Me3H3K27, a mark to impose stronger repression

Our results point to a novel, and tissue-specific, role of H3K27 methylation status for regulating T_3-response genes. The Polycomb repressive complex 2 is involved in Me3H3K27 acquisition (25) and the trithorax complex is involved in removing this mark (26). Little is known about their targeting mechanisms and their role in nuclear receptor function. To date, only Polycomb has been shown to be involved in regulation by the retinoic acid receptor (27). The present data show that H3K27 methylation has a strong impact on TR function. First, the high level of Me3H3K27 occupancy correlates with the lower expression of both genes in the tail fin compared with the brain without T_3. Second, the tail fin-specific, 5-fold decreases of Me3H3K27 after T_3 treatment correlate with the large induction mRNA levels induced by T_3. Me3H3K27 and Me3H3K4 are thought to be opposing modifications with regard to their consequences for gene activity (28). However, certain genes have been found to contain both marks simultaneously (28), with the repression function of Me3H3K27 dominating the activating Me3H3K4 modification (29). Most of these genes are poised for transcription, with preinitiated RNA PolII at their promoter and no Me3H3K36 on the transcribed DNA locus (30). This mechanism does not apply to *TRβ*. Interestingly, and consistently with our data for *TRβ*, these loci are transcribed at low levels (31). Furthermore, cobinding of HDAC1 and p300 at the promoter of a silent locus has been observed (31) as well as for *TRβ* T_3RE (10). A final possibility is that the two modifications do not co-occur within the same cell. Such a situation has been described for *Xenopus* (32).

H3K4 methylation status, a code to govern specificity of T_3-response gene regulation

Of all the histone modifications analyzed, the H3K4 methylation marks showed the strongest gene-specific pattern. The level of Me3H3K4 on the TRβ locus was constantly about 10 time higher than that of *TH/bZip*, and this high level was maintained despite T_3-induced changes in transcription. The presence of Me3H3K4 in premetamorphic tadpoles could either be independent of transcription initiation or be a historical mark of previous transcriptional initiation (30). T_3 decreases Me2H3K4 marks on *TRβ* gene, as observed for estrogen receptor with its ligand (33). The levels resulting from T_3 treatment are consistent with activation of transcription, because Me2H3K4 is totally absent on repressed targets (23). This selective variation might be dictated by the surrounding histone marks around the promoter. One such mark could be AcH3K9, known to block complete H3K4 demethylation (34). Thus, decreased Me2H3K4 occupancy without leading to gene repression could limit gene activation. Attenuation of promoter activation by Me2/Me3H3K4 was also recently described (35). Many histone methylations serve as recruitment marks for specific proteins, again limiting activation by implementation of enzymatic activities at the site of recruitment. *TH/bZIP* shows an unusual pattern, with absence of Me3H3K4 with or

without T_3 and an increase of Me2H3K4 after T_3 treatment. Whereas Me2H3K4 and Me3H3K4 are usually concordant at most genes, a subset of differentially methylated, Me2H3K4+/Me3H3K4− genes exist (36). The common feature of this gene category could be the presence of an enhancer region that imposes stricter control of initiation than that typically observed at other genes where transcription is controlled by initiation and elongation. Such a mechanism would fit with the tight repression of *TH/bZIP* in absence of T_3 and its strong activation with T_3.

TR binding and specificity of T_3-response gene regulation

In vitro studies in a variety of cell types from different vertebrate species show that TR binds to T_3RE independent of hormone presence. Given the significant levels of TRα expression in premetamorphic tadpoles (37), it is surprising to find first, no binding or very low binding of TR to the *TH/bZIP* T_3RE and second, increased binding of TR to both *TH/bZIP* and *TR*β T_3RE after addition of T_3. The abundance of TRα *vs.* TRβ and their specificity of DNA binding could account for such difference. Further studies will be necessary to address this point. TRβ level of expression alone does not appear to be responsible for the difference in TR occupancy before hormone treatment. In presence of T_3, the overexpression of TRβ leads to similar levels of TRβ binding on both *TR*β and *TH/bZIP* T_3RE, confirming the need of sufficient TRβ expression for binding to the *TH/bZIP* T_3RE (9) and suggesting that T_3 increases TRβ binding capacity. Thus, the type of T_3RE, *TR*β level of expression, and T_3 could all contribute to controlling TR binding.

These results are also pertinent to interpretation of the dual function model for the role of TR during amphibian development (37). In this model, T_3-response genes would be repressed by unliganded-TR during premetamorphosis, with T_3 playing a critical, activating role during metamorphosis. As TR binding was not detected on the *TH/bZIP* promoter during premetamorphosis, the very low levels of expression of *TH/bZIP* before metamorphosis would appear not to involve TR-dependent repression. However, TR binding to *TH/bZIP* T_3RE might be less stable or more dynamic, precluding detection by ChIP. Moreover, repression could also implicate other transcription factors. Moreover, some data support a working model in which initial unstable recruitment of silencing mediator of retinoid and TR/ nuclear receptor corepressor complexes via unliganded TR generates a histone code that serves to stabilize their own recruitment (38, 39) and thus to propagate repression (40).

Chromatin configuration also contributes to controlling TR binding. Levels of methylated H3K4 correlate with TR occupancy. Pharmacological modification of the methylation status of H3K4 confirmed these observations because increasing H3K4 methylation leads to an increase of TR binding at the T_3RE. Thus, H3K4 methylation could provide landmarks for high TR binding. A similar process has been described for estrogen receptor where histone H3K9 methylation modulates estrogen receptor binding to DNA in absence of 17β-estradiol (33). Because methylated H3K4 colocalizes with enhancer regions (41, 42), this mark could have a functional role for binding of transcription factors. This observation has considerable broad significance because a large number of putative sequences with regulatory elements characteristics can be found using bioinformatic tools, but not all of them bind transcription factors. Thus, combining sequence searches and chromatin landscape data will provide new opportunities to define true, functional regulatory elements. Now, the main question is what factors determine the presence of the methylation on H3K4 before metamorphosis. It is possible that DNA methylation is a downstream event to safeguard the silent status of a promoter (43). Future studies will be necessary to test this hypothesis and will complete this first *in vivo* analysis during vertebrate development for any nuclear receptors of the link between histone marks and T_3-response gene regulation or TR binding to DNA.

Materials and Methods

Animals and treatments

X. tropicalis adult frogs were obtained from NASCO (Fort Atkinson, WI) and maintained at 24 C in aquatic housing system (MPAquarien, Rockenhausen, Germany). Mating was induced by injection of 200 U of human chorionic gonadotropine for females and 100 U for males (Chorulon; Intervet, Beaucouze, France). Tadpoles were raised at 26 C. *X. laevis* frogs and tadpoles were raised as previously described (44). For T_3 treatment, tadpoles were maintained 48 h, in 5 liters with 10 nM T_3 (Sigma, St. Quentin Fallavier, France). The water was changed daily. Tadpoles were killed by decapitation after anesthesia (0.01% MS222, Sigma) before brain isolation and tail fin dissection. Tadpoles were staged according to the normal table of *X. laevis* (Daudin) of Nieuwkoop and Faber (45). Animal care was in accordance with institutional and national guidelines.

RNA isolation and RT-qPCR analysis

For each physiological conditions, brain or tail fin isolated from groups of 10 tadpoles were collected, flash frozen, and stored at −80 C. The tissue lysis was performed in 500 μl of RNAble (Gex-ex-T00–0U; Eurobio, Les Ulis, France) with one bead (INOX AISI 304 grade 100 AFBMA) using Tissue Lyser II apparatus (QIAGEN, Courtaboeuf, France) for 1 min at 30 Hz. The lysed tissues were mixed with chloroform and incubated on ice for 5 min before centrifugation (12,000 × *g*, 15 min, 4 C). The supernatant was subjected to RNA purification with RNeasy MinElute Cleanup kit according to manufacturer (ref :

74204, QIAGEN). RNA concentration was measured by optic density. RNA quality was estimated by microcapillary electrophoresis using Qiaxcel (QIAGEN). Potential contamination by genomic DNA was removed using DNAse treatment as described by the provider (Turbo DNA free; Ambion, Applied Biosystems, Courtaboeuf, France). Reverse transcription (RT) was done as previously described (37) using Superscript III reverse transcriptase (Invitrogen, Fisher Scientific, Illkirch, France). RT products were analyzed by real-time qPCR performed on an ABI 7300 (Applied Biosystems). Primers were designed using Primer express (Applied Biosystems). The list of used primers is given in Supplemental Table 1. Prism 7300 system software (Applied Biosystems) was used to analyze the results. In Fig. 1, the data are presented in means of Log($2^{-\Delta CT}$) and SEM (CT, cycle time). The raw data of three to six biological replicates are first normalized on the endogenous control gene *rpl8* (ΔCT: mean CT *rpl8* minus mean CT gene of interest) followed by Log transformation, so the variances between groups succeed the F test. In Fig. 6, the results are presented in fold increase (means and SEM). The raw data are normalized on the endogenous control gene *rpl8* and on the nontreated sample control by the $2^{-\Delta\Delta CT}$ method. For statistical analysis, the Log of the normalized data were (after Kolmogorov and Smirnov normality test) subjected to a one-sample two-tailed *t* test ($\alpha = 5\%$).

ChIP and qPCR analysis

Dissected brains or tail fins, up to 30 to 50 mg, from seven euthanized tadpoles were used to isolate chromatin. ChIP was done as previously described (46) with slight modifications. ChIP products were analyzed by real-time qPCR as previously described for RT products analysis. Primers are given in Supplemental Fig. 1. The results were expressed as percent of input and presented as means SEM of at least four independent experiments. Statistical analyses were performed with a paired one-tailed *t* test ($\alpha = 5\%$). A detailed procedure is presented in Supplemental Fig. 8.

Antibodies

Antibody against TR was previously described and used in ChIP assay (37). Antibody against RNA PolII (CTD4H8) was from Epigentec (A-2032; Euromedex, Souffelweyersheim, France). All the antibodies against chromatin modifications pan-AcH4 (06-866), AcH3K9 (07-352), AcH3K18 (07-354), Me2H3K4 (07-030), Me3H3K4 (07-473), Me2H3K9 (07-441), Me3H3K9 (17-625), and Me3H3K27 (17-622) were from Upstate Biotechnology (Millipore, Saint-Quentin en Yvelines, France). Antibody against Me3H3K36 (ab1785) was from Abcam (Paris, France). Antibody against GFP was from Torrey Pines Biolabs (CliniSciences, Montrouge, France).

Transgenesis

F_0 transgenic animals were generated by restriction enzyme-mediated integration nuclear transplantation (47) with slight modifications (16). The introduced DNA is a plasmid expressing the *X. laevis* TRβ protein fused to the C-terminal part of GFP from the cytomegalovirus promoter (16) or from neurotubulin β (NβT) promoter. The NβT-GFP-TRβ construct was generated by inserting the GFP-TRβ AgeI-DraIII insert in front of the NβT promoter of the NβT-GFP construct previously described (15). where the cytomegalovirus promoter was replaced by the NβT promoter. To select founder transgenic animals, fluorescent proteins were observed on anesthetized (0.01% MS222) intact embryos and latter tadpoles, under a dissecting scope equipped with fluorescent light. F_0 generation was used to investigate and confirm the functionality of the GFP-fused TRβ protein compared with TRβ wild-type protein as well as the comparable levels of expression between groups of transgenic animals (16). F_1 generation was used for ChIP assay analysis. Mating with two transgenic animals was induced by injection of 500 U of human chorionic gonadotropine for females and 200 U for males. F_1 transgenic tadpoles with similar level of GFP expression were carefully selected as F_0 tadpoles.

Tail culture

Tail cultures was done as previously described (23). Samples were placed in culture dishes (12-well plates) containing the culture medium and maintained at 24 C. The tails were treated for 48 h with or without 10 nM T_3 (Sigma) and/or 0.1 mM Pargylin (P8013, Sigma) immediately at the start of the culture. Prior chromatin extraction and RNA isolation tail fins were isolated.

Acknowledgments

We thank Dr. M.-S. Clerget-Froidevaux (Paris), G. Morvan-Dubois (Paris), D. Buchholz (Cincinnati) and S. Ait.Si.Ali (Paris) for helpful discussions during the progression of this study. We also thank J.-P. Chaumeil (Paris) and G. Benisti (Paris) for animal care.

Address all correspondence and requests for reprints to: Laurent M. Sachs, Unité Mixte de Recherche 7221 Centre National de la Recherche Scientifique, Muséum National d'Histoire Naturelle, Case Postale 32, 7 rue Cuvier, 75231 Paris cedex 05, France. E-mail: sachs@mnhn.fr.

This work was supported by the Centre National de la Recherche Scientifique, the Muséum National d'Histoire Naturelle, the European Coordinated Action XOMICS, the European Network of Excellence CASCADE (contract no. FOOD-CT-2004-506319), CRESCENDO, an Integrated Project funding from Framework Programme 6 (contract no. LSHM-CT-2005-018652), SIGNATOR (Agence National pour la Recherche ANR-06-BLAN-0232-01), and TRIGGER (ANR-08-JCJC-0100-01. A CIFRE grant and the WatchFrog Co. supported P.B.

Present address for E.H.: Université Pierre et Marie Curie, Paris 06, Centre National de la Recherche Scientifique, Unité Mixte de Recherche 7622, 75005 Paris cedex 05, France.

Disclosure Summary: B.A.D was consultant for WatchFrog in 2008 and is member of the Centre National de la Recherche Scientifique advisory council. P.B. was employed by WatchFrog Co. (Evry, France). The other authors have nothing to disclose.

References

1. **Mangelsdorf DJ, Thummel C, Beato M, Herrlich P, Schütz G, Umesono K, Blumberg B, Kastner P, Mark M, Chambon P, Evans RM** 1995 The nuclear receptor family: the second decade. Cell 83:835–839
2. **Strahl BD, Allis CD** 2000 The language of covalent histone modifications. Nature 403:41–45
3. **Wolffe AP** 1997 Transcriptional control. Sinful repression. Nature 387:16–17

4. **Huang ZQ, Li J, Sachs LM, Cole PA, Wong J** 2003 A role for cofactor-cofactor and cofactor-histone interactions in targeting p300, SWI/SNF and mediator for transcription. EMBO J 22:2146–2155
5. **Shi YB** 1999 Amphibian metamorphosis. From morphology to molecular biology. New York: John Wiley & Sons
6. **Brown DD, Cai L** 2007 Amphibian metamorphosis. Dev Biol 306:20–33
7. **Wang X, Matsuda H, Shi YB** 2008 Developmental regulation and function of thyroid hormone receptors and 9-cis retinoic acid receptors during *Xenopus tropicalis* metamorphosis. Endocrinology 149:5610–5618
8. **Das B, Heimeier RA, Buchholz DR, Shi YB** 2009 Identification of direct thyroid hormone response genes reveals the earliest gene regulation programs during frog metamorphosis. J Biol Chem 284:34167–34178
9. **Buchholz DR, Paul BD, Shi YB** 2005 Gene-specific changes in promoter occupancy by thyroid hormone receptor during frog metamorphosis. Implications for developmental gene regulation. J Biol Chem 280:41222–41228
10. **Havis E, Sachs LM, Demeneix BA** 2003 Metamorphic T3-response genes have specific co-regulator requirements. EMBO Rep 4:883–888
11. **Ranjan M, Wong J, Shi YB** 1994 Transcriptional repression of *Xenopus* TR β gene is mediated by a thyroid hormone response element located near the start site. J Biol Chem 269:24699–24705
12. **Furlow JD, Brown DD** 1999 *In vitro* and *in vivo* analysis of the regulation of a transcription factor gene by thyroid hormone during *Xenopus laevis* metamorphosis. Mol Endocrinol 13:2076–2089
13. **Andersen CL, Jensen JL, Ørntoft TF** 2004 Normalization of real-time quantitative reverse transcription-PCR data: a model-based variance estimation approach to identify genes suited for normalization, applied to bladder and colon cancer data sets. Cancer Res 64:5245–5250
14. **Schreiber AM, Das B, Huang H, Marsh-Armstrong N, Brown DD** 2001 Divers developmental programs of *Xenopus laevis* metamorphosis are inhibited by a dominant negative thyroid hormone receptor. Proc Natl Acad Sci USA 98:10739–10744
15. **Coen L, du Pasquier D, Le Mevel S, Brown S, Tata J, Mazabraud A, Demeneix BA** 2001 *Xenopus* Bcl-X(L) selectively protects Rohon-Beard neurons from metamorphic degeneration. Proc Natl Acad Sci USA 98:7869–7874
16. **Havis E, Le Mevel S, Morvan Dubois G, Shi DL, Scanlan TS, Demeneix BA, Sachs LM** 2006 Unliganded thyroid hormone receptor is essential for *Xenopus laevis* eye development. EMBO J 25:4943–4951
17. **Bannister AJ, Schneider R, Myers FA, Thorne AW, Crane-Robinson C, Kouzarides T** 2005 Spatial distribution of di- and tri-methy lysine 36 of histone H3 at active genes. J Biol Chem 280:17732–17736
18. **Martin C, Zhang Y** 2005 The diverse functions of histone lysine methylation. Nat Rev Mol Cell Biol 6:838–849
19. **Ruthenburg AJ, Allis CD, Wysocka J** 2007 Methylation of lysine 4 on histone H3: intricacy of writing and reading a single epigenetic mark. Mol Cell 25:15–30
20. **Swigut T, Wysocka J** 2007 H3K27 demethylases, at long last. Cell 131:29–32
21. **Hublitz P, Albert M, Peters AHFM** 2009 Mechanisms of transcriptional repression by histone lysine methylation. Int J Dev Biol 53:335–354
22. **Metzger E, Wissmann M, Yin N, Müller JM, Schneider R, Peters AH, Günther T, Buettner R, Schüle R** 2005 LSD1 demethylates repressive histone marks to promote androgen-receptor-dependent transcription. Nature 437:436–439
23. **Shi Y, Lan F, Matson C, Mulligan P, Whetstine JR, Cole PA, Casero RA, Shi Y** 2004 Histone demethylation mediated by the nuclear amine oxidase homolog LSD1. Cell 119:941–953
24. **Sachs LM, Amano T, Shi YB** 2001 An essential role of histone deacetylases in postembryonic organ transformations in *Xenopus laevis*. Int J Mol Med 8:595–601
25. **Cao R, Wang L, Wang H, Xia L, Erdjument-Bromage H, Tempst P, Jones RS, Zhang Y** 2002 Role of histone H3 lysine 27 methylation in Polycomb-group silencing. Science 298:1039–1043
26. **Cloos PA, Christensen J, Agger K, Helin K** 2008 Erasing the methyl mark : histone demethylases at the center of cellular differentiation and disease. Genes Dev 22:1115–1140
27. **Gillespie RF, Gudas LJ** 2007 Retinoid regulated association of transcriptional co-regulators and the Polycomb group protein SUZ12 with the retinoic acid response elements of Hoxa1, RARβ(2), and Cyp26A1 in F9 embryonal carcinoma cells. J Mol Biol 372:298–316
28. **Bernstein BE, Mikkelsen TS, Xie X, Kamal M, Huebert DJ, Cuff J, Fry B, Meissner A, Wernig M, Plath K, Jaenisch R, Wagschal A, Feil R, Schreiber SL, Lander ES** 2006 A bivalent chromatin structure marks key developmental genes in embryonic stem cells. Cell 125:315–326
29. **Yu H, Zhu S, Zhou B, Xue H, Han JDJ** 2008 Inferring causal relationships among different histone modifications and gene expression. Genome Res 18:1314–1324
30. **Guenther MG, Levine SS, Boyer LA, Jaenisch R, Young RA** 2007 A chromatin landmark and transcription initiation at most promoters in human cells. Cell 130:77–88
31. **Stock JK, Giadrossi S, Casanova M, Brookes E, Vidal M, Koseki H, Brockdorff N, Fisher AG, Pombo A** 2007 Ring-1 mediated ubiquitination of H2A restrains poised RNA polymerase II at bivalent genes in mouse ES cells. Nat Cell Biol 9:1428–1435
32. **Akkers RC, van Heeringen SJ, Jacobi UG, Janssen-Megens EM, Françcoijs KJ, Stunnenberg HG, Veenstra GJ** 2009 A hierarchy of H3K4me3 and H3K27me3 acquisition in spatial gene regulation in *Xenopus* embryos. Dev Cell 17:425–434
33. **Garcia-Bassets I, Kwon YS, Telese F, Prefontaine GG, Hutt KR, Cheng CS, Ju BG, Ohgi KA, Wang J, Escoubet-Lozach L, Rose DW, Glass CK, Fu XD, Rosenfeld MG** 2007 Histone methylation-dependent mechanisms impose ligand dependency for gene activation by nuclear receptors. Cell 128:505–518
34. **Forneris F, Binda C, Dall'Aglio A, Fraaije MW, Battaglioli E, Mattevi A** 2006 A highly specific mechanism of histone H3–K4 recognition by histone demethylase LSD1. J Biol Chem 281:35289–35295
35. **Pinskaya M, Gourvennec S, Morillon A** 2009 H3 lysine 4 di- and tri-methylation deposited by cryptic transcription attenuates promoter activation. EMBO J 28:1697–1707
36. **Orford K, Kharchenko P, Lai W, Dao MC, Worhunsky DJ, Ferro A, Janzen V, Park PJ, Scadden DT** 2008 Differential H3K4 methylation identifies developmentally poised hematopoietic genes. Dev Cell 14:798–809
37. **Sachs LM, Shi YB** 2000 Targeted chromatin binding and histone acetylation in vivo by thyroid hormone receptor during amphibian development. Proc Natl Acad Sci USA 97:13138–13143
38. **Yu J, Li Y, Ishizuka T, Guenther MG, Lazar MA** 2003 A SANT motif in the SMRT corepressor interprets the histone code and promotes histone deacetylation. EMBO J 22:3403–3410
39. **Yoon HG, Choi Y, Cole PA, Wong J** 2005 Reading and function of a histone code involved in targeting corepressor complexes for repression. Mol Cell Biol 25:324–335
40. **Hartman HB, Yu J, Alenghat T, Ishizuka T, Lazar MA** 2005 The histone-binding code of nuclear receptor co-repressors matches the substrate specificity of histone deacetylase 3. EMBO Rep 6:445–451
41. **Heintzman ND, Hon GC, Hawkins RD, Kheradpour P, Stark A, Harp LF, Ye Z, Lee LK, Stuart RK, Ching CW, Ching KA, Antosiewicz-Bourget JE, Liu H, Zhang X, Green RD, Lobanenkov VV, Stewart R, Thomson JA, Crawford GE, Kellis M, Ren B** 2009

Histone modifications at human enhancers reflect global cell-type-specific gene expression. Nature 459:108–112
42. **He HH, Meyer CA, Shin H, Bailey ST, Wei G, Wang Q, Zhang Y, Xu K, Ni M, Lupien M, Mieczkowski P, Lieb JD, Zhao K, Borwn M, Liu XS** 2010 Nucleosome dynamics define transcriptional enhancers. Nat Genet 42:343–347
43. **Okitsu CY, Hsieh CL** 2007 DNA methylation dictates histone H3K4 methylation. Mol Cell Biol 27:2746–2757
44. **de Luze A, Sachs L, Demeneix B** 1993 Thyroid hormone-dependent transcriptional regulation of exogenous gene transferred into *Xenopus* tadpole muscle in vivo. Proc Natl Acad Sci USA 90:7322–7326
45. **Nieuwkoop PD, Faber J** 1956 Normal table of *Xenopus laevis* (Daudin). Amsterdam: Elsevier North Holland Publishing Company
46. **Froidevaux MS, Berg P, Seugnet I, Decherf S, Becker N, Sachs LM, Bilesimo P, Nygård M, Pongratz I, Demeneix BA** 2006 The co-chaperone XAP2 is required for activation of hypothalamic thyrotropin-releasing hormone transcription in vivo. EMBO Rep 7:1035–1039
47. **Kroll KL, Amaya E** 1996 Transgenic *Xenopus* embryos from sperm nuclear transplantations reveal FGF signaling requirements during gastrulation. Development 122:3173–3183